Photo-emission of two protons from nuclei

Marta Anguiano[1], Giampaolo Co'[2,3] and Antonio M. Lallena[4]

[1] Departamento de Radiación Electromagnética, Instituto de Física Aplicada, CSIC, Serrano 144, E-28006 MADRID, Spain

[2] Dipartimento di Fisica, Università di Lecce, I-73100 Lecce, Italy

[3] Istituto Nazionale di Fisica Nucleare sez. di Lecce, I-73100 Lecce, Italy

[4] Departamento de Física Moderna, Universidad de Granada, E-18071 Granada, Spain

The photo-emission of two protons from the ^{12}C, ^{16}O and ^{40}Ca nuclei is investigated. Aim of the work is the study of the possibilities offered by this probe to obtain information about the characteristics of the short-range correlations. We have also evaluated the effects of the two-body Δ-currents which, in this processes, compete with those produced by the short-range correlations. Our results show that (γ,pp) processes could be more useful than (e,e'pp) for the study of the short-range correlations.

1. Introduction

This article belongs to a series dedicated to the study of the Short Range Correlations (SRC) effects in processes induced by electromagnetic probes on atomic nuclei. We have already conducted this study for inclusive electron scattering [1, 2, 3], (e,e'p) [4], (γ,p) [5] and (e,e'pp) [6] reactions. In this work we investigate the (γ,pp) case.

Inclusive and one-nucleon emission processes are dominated by the uncorrelated one-body responses. Our results [1, 2, 3, 4, 5] show that the SRC produce small corrections to the uncorrelated cross sections. The size of these corrections remains within the theoretical uncertainties due to the arbitrary choice of the input parameters.

The emission of two nucleons cannot be induced by uncorrelated one-body operators. For this reason these processes are the ideal tool to study the SRC effects. However, even in this case the situation is not completely clean, since two nucleons can also be emitted by two-body Meson-Exchange Currents (MEC) without any contribution of the SRC. The most important MEC terms, called seagull and pionic, are produced by the exchange of charged pions. When the two emitted nucleons are of the same type, for example two protons, these terms do not act. For this reason the MEC contribution in the emission of a proton-neutron pair is noticeably larger than in the case of nucleon-like emission [7, 8]. In this last case the active MEC terms, where a single uncharged meson is exchanged, are due to the virtual excitations of the Δ resonance [9].

In principle the contribution of the MEC could be eliminated by a super Rosenbluth separation of the (e,e'pp) cross section. With this procedure it is possible to extract the longitudinal (charge) response, where the MEC effects are negligible [10], therefore the signature of the SRC would be very clean.

From the experimental point of view the Rosenbluth separation is extremely difficult. We think it is more fruitful to study the effects of the the Δ currents in order to keep them under control. In [6] this investigation has been done for (e,e'pp) processes, and in the present paper we continue it for the case of real photons. Real photons have less flexibility than electrons, because the momentum transferred to the nucleus is fixed by the energy of the absorbed photons. On the other hand, since they are purely transverse, the longitudinal terms are not present in the cross section, and this simplifies the analysis of the results.

In recent years theoretical studies of the emission of two nucleons induced by the absorption of real photons have been done by the Valencia [11], Pavia [12, 13] and Gent

[14] groups. The Valencia model is based on a Fermi gas description of the nucleus, i.e. all the single particle wave functions are plane waves. The final state interactions (FSI) are calculated by explicitly considering the various diagrams that describe the interaction of the emitted nucleons with the rest nucleus. Our approach is more similar to that of the Pavia group which uses Woods-Saxon single particle wave functions and complex optical potentials to treat FSI. The difference in the two models is in the treatment of the SRC. The Pavia group uses two-nucleon spectral functions, while we make an expansion of the transition matrix elements in power of the correlation function (see section 2). The Gent group uses single particle wave functions generated by Hartree-Fock calculations. FSI are considered within a self-consistent continuum Random Phase Approximation framework.

The experimental situation is very promising. Data have been taken at various laboratories [15] and have shown the feasibility of these experiments with the present facilities. Furthermore, they have clearly indicated the different sensitivities of (γ,pn) and (γ,pp) reactions to the SRC and MEC. A direct comparison between our results and the available data is not straightforward, since the data have been averaged on the energy and angular acceptances of the nucleon detectors; also a certain range of the energy of the incident photons has been considered. For this reason we postpone this comparison, requiring a direct contact with the experimental groups, to eventual forthcoming publications.

In this paper after summarizing in section 2 the basic formulas used to describe (γ,pp) processes with our model, we discuss the results obtained for the ^{12}C, ^{16}O and ^{40}Ca nuclei aimed to understand our capacity of keeping under control the Δ currents and to investigate the SRC characteristics.

2. The cross section

In this section we briefly recall the expressions used in our calculations to describe the (γ,pp) cross section. A more detailed derivation of the cross section expression can be found in [16], while our nuclear model has been widely described in [6].

We label the energy and momentum of the photon as ω and $\mathbf{q}$, respectively, and the four momenta of the emitted nucleons with $p_1 \equiv (\epsilon_1, \mathbf{p}_1)$ and $p_2 \equiv (\epsilon_2, \mathbf{p}_2)$. The kinematics set up

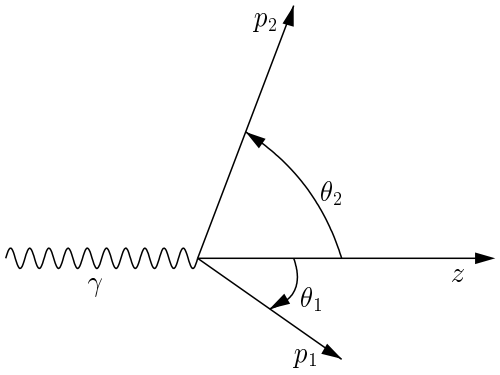

Figure 1. Reference system used in our calculations. The z axis indicates the direction of $\mathbf{q}$, the photon momentum. The vectors $\mathbf{q}$, $\mathbf{p}_1$ and $\mathbf{p}_2$ are on the same plane. The arrows of the angles θ_1 and θ_2 indicates the direction of their positive values.

is defined in Fig. 1. The directions of the two emitted nucleons can be identified by the angles formed with the photon direction. We call these angles θ_1 and θ_2, and define $\theta_{12} = \theta_1 - \theta_2$. The figure shows that, in our representation, the two angles are defined positive in opposite directions with respect to z-axis.

In natural units ($\hbar = c = 1, e^2 = 1/137.04$), the expression of the cross section we adopt is:

$$\frac{\mathrm{d}^5\sigma}{\mathrm{d}\Omega_1 \mathrm{d}\epsilon_2 \mathrm{d}\Omega_2} = \frac{K}{(2\pi)^6} \frac{2\pi^2 e^2}{\omega} f_{\mathrm{rec}}\, w_t(|\mathbf{q}|)\,, \tag{1}$$

where e is the elementary charge. In the above equation, K is a kinematic factor

$$K = m^2\, |\mathbf{p}_1|\, |\mathbf{p}_2|\,, \tag{2}$$

and f_{rec} is a recoil factor defined as:

$$f_{\mathrm{rec}}^{-1} = 1 + \frac{m}{M_{A-2}} \left[1 + \frac{|\mathbf{p}_1|}{|\mathbf{p}_2|} \cos\theta_{12} - \frac{|\mathbf{q}|}{|\mathbf{p}_2|} \cos\theta_2\right]\,, \tag{3}$$

where m is the proton mass and M_{A-2} the mass of the rest nucleus.

The nuclear structure information is included in the w_t factor

$$\begin{aligned} w_t(|\mathbf{q}|) = {} & \langle\Psi_i|J_-^\dagger(\mathbf{q})|\Psi_f\rangle \langle\Psi_f|J_-(\mathbf{q})|\Psi_i\rangle \\ & + \langle\Psi_i|J_+^\dagger(\mathbf{q})|\Psi_f\rangle \langle\Psi_f|J_+(\mathbf{q})|\Psi_i\rangle\,, \end{aligned} \tag{4}$$

where we have indicated with $|\Psi_i\rangle$ and $|\Psi_f\rangle$ the initial and final states of the full hadronic system. We do not consider the polarization of the emitted nucleons, therefore in the previous equations a sum on the third components of the spin of the emitted particles and of the angular momentum of the residual nucleus is understood.

The operators present in Eq. (4) are the transverse components of the electromagnetic four-current operator composed by one- and two-body terms. The one-body electromagnetic currents are produced by the convection current,

$$J^{\mathrm{C}}(\mathbf{r}) = \sum_{k=1}^{A} \frac{-i}{2m_k} \frac{1+\tau_k^3}{2} \left[\delta(\mathbf{r}-\mathbf{r}_k)\nabla_k - \nabla_k \delta(\mathbf{r}-\mathbf{r}_k)\right]\,, \tag{5}$$

and by the magnetization current,

$$J^{\mathrm{M}}(\mathbf{r}) = \sum_{k=1}^{A} \frac{1}{2m_k} \left(\mu^{\mathrm{P}} \frac{1+\tau_k^3}{2} + \mu^{\mathrm{N}} \frac{1-\tau_k^3}{2}\right) \nabla \times \delta(\mathbf{r}-\mathbf{r}_k)\, \boldsymbol{\sigma}_k\,. \tag{6}$$

In the previous equations m_k indicates the mass of k–th nucleon, μ^{P} and μ^{N} the anomalous magnetic moment of the proton and of the neutron respectively, $\boldsymbol{\sigma}_k$ the Pauli spin matrix of the k-th nucleon and $\tau_k^3 = 1$ (-1) in case the k-th nucleon is a proton (neutron). In our calculations the internal structure of the nucleon has been considered by folding the point-like responses with the electromagnetic nucleon form factors of [17].

We point out that, in the present article, we have considered the convection current which was not included in the calculation of [6]. We have shown in [5] that the contribution of the convection current is relevant for the photoabsorption processes, while it is negligible for electron scattering in the quasi-elastic region.

We have already mentioned in the introduction that, since we have considered only the emission of two like particles, specifically two protons, the two-body currents induced by the exchange of charged mesons do not contribute. The main two-body current contribution arises from diagrams like those of Fig. 2 where the exchanged π meson is chargeless. We describe these Δ currents following the prescription of [18]. The corresponding expressions in

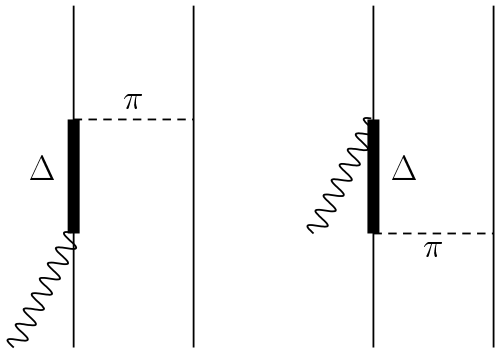

Figure 2. Meson exchange current diagrams considered in our calculations. The wavy lines represent the photon, and the full lines the nucleons. Since we describe the emission of two protons, the exchanged pion is chargeless.

our approach are given in [6]. We would like to mention here that these currents depend on the product of the three coupling constants related to the three vertexes of the diagrams of Fig. 2. They are: the pion-nucleon coupling constant $f_{\pi NN}$, the pion-nucleon-delta coupling constant $f_{\pi N\Delta}$, and, finally, the photon-nucleon-delta coupling constant $f_{\gamma N\Delta}$. Out of these three constants only $f_{\pi NN}$ is rather well determined by the experimental data. Its commonly accepted value is $f^2_{\pi NN}/4\pi$=0.079. We used the uncertainty on the values of the other constants to estimate the sensitivity of our results to the two-body Δ currents.

The calculation of the nuclear response (4) requires a model for nuclear states. A detailed description of our model can be found in [6], and here we recall some of the basic ideas and approximations.

The nuclear states are described as:

$$|\Psi\rangle \;=\; \frac{F|\Phi\rangle}{\langle\Phi|F^+F|\Phi\rangle}\,. \tag{7}$$

In the above expression $|\Phi\rangle$ is a Slater determinant formed by single particle states generated by a one-body hamiltonian, which in our calculations is obtained by using a Woods-Saxon potential well. The ground state is described by using the ground state Slater determinant, formed by all, and only, the states whose single particle energies are smaller than the Fermi energy. The excited states are described as Slater determinants formed by two-particle two-hole excitations. The two particle states are continuum single particle wave functions, calculated as scattering waves from the mean-field potential.

The ingredient making possible the two-nucleon emission by one-body operators, is the correlation function F. In our calculations we have used purely scalar correlations defined as:

$$F(1,2,...A) \;=\; \prod_{i<j}^{A} f(r_{ij})\,, \tag{8}$$

where $r_{ij} = |\mathbf{r}_i - \mathbf{r}_j|$ is the distance between the particles i and j. The insertion of Eq. (7) in the expression (4) allows us to make an expansion in terms of the function $h_{ij} = f^2(r_{ij}) - 1$. The main approximation of our model consists, in retaining only those terms of the expansion where the function h_{ij} appears only once.

At this point, it may be worth to mention two properties related to the presence of the denominator in Eq. (7). The first, and more relevant one from the physics point of view, is that the denominator ensures the proper normalization of the many-body correlated wave function. The second property is more technical, but still relevant. The denominator cancels all the unlinked terms of the expansion in terms of h_{ij} [19]. Only after making this cancellation we cut the expansion to the first order in h_{ij}.

This model has been developed to calculate the ground state densities and momentum distributions [20, 21], and later extended to describe the nuclear excited states [1, 2, 3, 4, 5, 6]. The validity of the truncation procedure has been tested in nuclear matter against a calculation where all the power terms in h_{ij} have been considered [22]. The quasi-elastic charge responses obtained with the two methods are in excellent agreement.

3. Results

The kinematics of the process is such that energy and momentum conservations imply:

$$\omega = \frac{\mathbf{p}_1^2}{2m} + \frac{\mathbf{p}_2^2}{2m} - \epsilon_{h_1} - \epsilon_{h_2} + \frac{\mathbf{p}_r^2}{2M_{A-2}}\,, \tag{9}$$

$$\mathbf{q} = \mathbf{p}_1 + \mathbf{p}_2 + \mathbf{p}_r \ , \tag{10}$$

where, we have considered non relativistic kinematics, and we have indicated with ϵ_{h_1} and ϵ_{h_2} the single particle energies of the levels where the two protons are emitted from, and with $\mathbf{p}_r$ the recoil momentum of the remaining nucleus. The other variables have been defined in the previous section.

Our calculations have been done for fixed values of ω, $\mathbf{q}$ and $\epsilon_2 = \mathbf{p}_2^2/2m$ and θ_2 By selecting the final state of the rest nucleus, also ϵ_{h_1} and ϵ_{h_2} are fixed. The labels indicating the two-hole compositions of the nuclear final states of the reactions we have considered in our calculations, are given in Table 1. We calculate the cross section as a function of θ_1, and for each value of this angle, $|\mathbf{p}_r|$ and $|\mathbf{p}_1|$ are obtained by solving the system formed by Eqs. (9) and (10), this last one squared. This calculation is quite involved since it should be repeated, for every θ_1, with a different single particle wave function which depends from $\epsilon_1 = \mathbf{p}_1^2/2m_1$. To relieve the numerical load we used an approximation, called no-recoil approximation (NRA) in [6]. The NRA consists in considering the mass of the A-2 nucleus heavy enough to neglect its recoiling energy in Eq. (9). In this case we have:

$$|\mathbf{p}_1| = \sqrt{2m(\omega - \epsilon_2 + \epsilon_{h_1} + \epsilon_{h_2})} \tag{11}$$

independent from θ_1. The value of $|\mathbf{p}_r|$ is then extracted by squaring Eq. (10).

	^{12}C	^{16}O	^{40}Ca
0_1^+	$(1p3/2)^{-2}$	$(1p1/2)^{-2}$	$(1d3/2)^{-2}$
0_2^+		$(1p3/2)^{-2}$	$(2s1/2)^{-2}$
1^+		$(1p1/2)^{-1}\ (1p3/2)^{-1}$	$(1d3/2)^{-1}\ (2s1/2)^{-1}$
2_1^+	$(1p3/2)^{-2}$	$(1p1/2)^{-1}\ (1p3/2)^{-1}$	$(1d3/2)^{-2}$
2_2^+		$(1p3/2)^{-2}$	$(1d3/2)^{-1}\ (2s1/2)^{-1}$

Table 1. Two-hole compositions of the nuclear final states for the (γ,pp) reactions we have considered.

The validity of the NRA has been discussed in [6], where we have shown that significant differences between the results of the exact calculations and those obtained within the NRA appear only in the minima of the cross section angular distribution. We have obtained analogous results for the (γ,pp) reactions. For the purposes of the present investigation the accuracy of NRA is sufficient, while an eventual comparison with experimental data would require the more accurate treatment of the kinematics.

As in [6], the hole single particle wavefunctions are obtained by using a real Woods-Saxon potential whose parameters have been fixed to reproduce charge density distributions and single particle energies close to the Fermi level. There is a certain degree of arbitrariness in this choice, since there are various parameterizations able to describe these data with the same degree of accuracy. We have verified that this uncertainty produces on our (γ,pp) cross sections variations of few percent. This is the same order of magnitude of the uncertainty found for the (e,e'pp) case [6].

The continuum single particle wave functions, have been described by using the complex optical potential of [23], which was fixed to reproduce elastic nucleon-nucleus cross section data. In our case this complex potential takes into account the re-scattering of the emitted nucleon with the rest nucleus. The interaction between the two emitted nucleons is neglected. Recent calculations [13] indicate that, for photons and for the kinematics we have chosen, this effect is negligible. The uncertainty on the choice of the continuum wave functions produce large effects on the cross section, and this fact deserves a more detailed discussion than for the bound wave functions. In Fig. 3 we show the results of the ^{16}O(γ,pp)^{14}C cross sections calculated with different sets of continuum wave functions, for the final state 0^+_1 (see Table 1). In the panel (a) of this figure, we show the cross sections as a function of the θ_1 angle. In these calculations the energy and the angle of the other emitted proton have been fixed as ϵ_2 = 40 MeV and $\theta_2 = 180^o$. The full line shows the result obtained by using the wavefunctions obtained with the optical potential of Schwandt et al. [23]. This is the potential we have used all along the remaining of the paper. A different parameterization of an optical potential also aiming to reproduce elastic scattering proton-nucleus data, is that of Nadasen et al. [24]. The dashed line of panel (a) shows the result obtained with this optical potential. The dotted line shows the result obtained by using, for the particle states, the same real Woods-Saxon potential adopted for the hole states. The parameters of this potential can be found in [25].

As it is well know, the imaginary part of the optical potential reduces the cross section. The use of these potentials is necessary to have a good description of single nucleon emission processes [16]. In this approach the hole and particle wave functions are not any more orthogonal. The effects of this non-orthogonality have been investigated in [26] and have been found to be small in the kinematic region we consider.

The number of the kinematic variables involved in the cross section calculations is quite large, therefore we checked the range of validity of our results by repeating the calculations under different kinematic conditions. Quite often the details of the angular distribution of the cross section are not relevant for our discussion We found useful to study the integrated cross section defined as:

$$S = \int \mathrm{d}\theta_1 \sin\theta_1 \frac{\mathrm{d}^5\sigma(\theta_1)}{\mathrm{d}\Omega_1 \mathrm{d}\epsilon_2 \mathrm{d}\Omega_2} \,. \tag{12}$$

which summarizes the global differences between the various calculations.

The integrated cross sections S have been calculated with the sets of single particle wave functions discussed above for $\theta_2 = 180^o$ and various values of the energy ϵ_2. The results of these calculations are shown in the panel (b) of Fig. 3 as a ratios of the S variables calculated with Nadasen and real Woods-Saxon potential divided by those obtained with the

Schwandt potential. It is evident that the behaviour shown in panel (a) is a general feature of the calculation. FSI reduce the cross sections, and the two optical potentials produce very similar results.

We have also investigated the effects of special kinematics on the FSI. Specifically we have chosen the super parallel back-to-back kinematics. In this case one proton is emitted in the direction of the momentum transfer and the other one in the opposite direction. We set $\theta_1 = 0^o$ and $\theta_2 = 180^o$. The kinematics is changed by modifying the energies of the emitted protons. An easy way to represent the cross sections in this case is to use $|\mathbf{p}_r|$ defined in Eq. (10). For fixed emission angles, the same value of this quantity can be obtained for two sets of energy values of the two emitted protons. In the superparallel back-to-back kinematics we can distinguish when $\mathbf{p}_r$ points in the direction of the momentum transfer $\mathbf{q}$ or in opposite

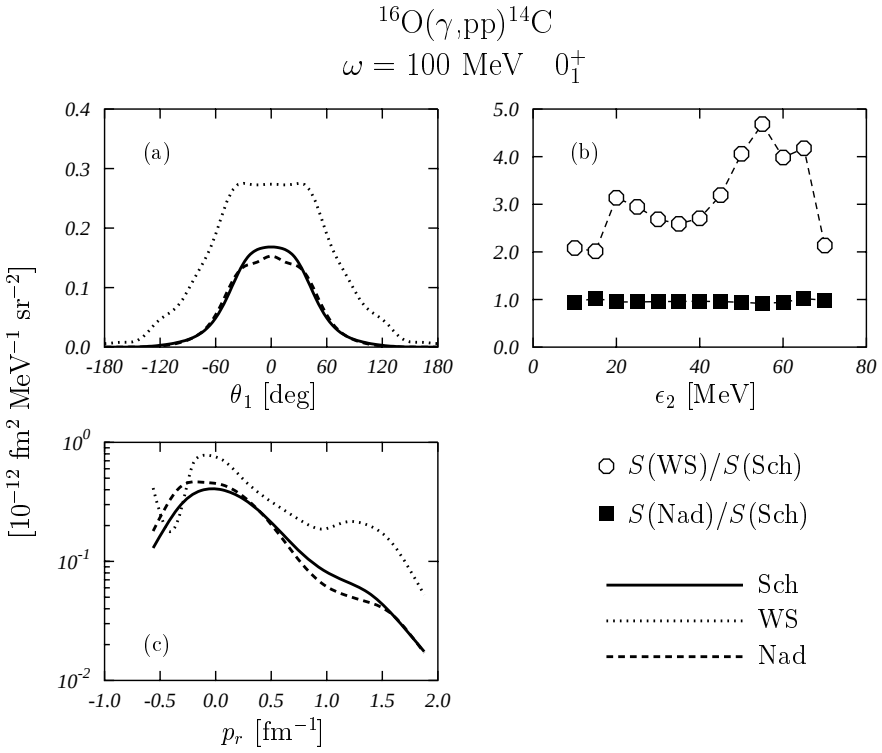

Figure 3. Two-nucleon emission cross sections on ^{16}O leading to the ^{14}C ground state. Panel (a): Dependence on the angle θ_1 of the first emitted proton, while the energy ϵ_2 of the other proton is fixed at 40 MeV and $\theta_2 = 180^o$. The full line shows the result obtained with the optical potential of Schwandt et al. [23], the dashed line with that of Nadasen et al. [24], while the dotted line has been obtained by using for the particle states the same real Woods-Saxon well used to generate the hole single particle wave functions. Panel (b): Ratios between S variables, Eq. (12) calculated with real Woods-Saxon well (WS), Nadasen potential (Nad) and Scwhandt potential (Sch). The lines have been drawn to guide the eyes. Panel (c): Cross sections in superparallel back-to-back kinematics. The variable $|\mathbf{p}_r|$ has been modified by changing the energies of the emitted nucleons, and it has been defined positive when it points in the direction of the momentum transfer $\mathbf{q}$. The meaning of the lines is the same as in the panel (a).

direction. We decided to assign positive values to $|\mathbf{p}_r|$ in the first case, and negative in the second one. For other kinematic set ups the use of $|\mathbf{p}_r|$ is more ambiguous.

The panel (c) of Fig. 3 shows the cross sections calculated for the kinematics described above with the potentials we are discussing. As expected the real Woods-Saxon potential produce larger cross sections, while the two optical potentials produce very similar cross section. We have calculated the values of the cross sections integrated in $\mathbf{p}_r$ and taken the ratios. We found a value of 2.06 for WS over Schwandt and 1.09 for Nadasen over Schwandt. The first value should be compared with the open circles of panel (b), and it is of the same order of the smallest values shown in the figure. The other value should instead be compared with the squares of panel (b). It is slightly larger than those shown. These results do not present any indication that FSI are reduced in superparallel back-to-back kinematics.

This investigation has been conducted also for the other ^{16}O states listed in the Table 1, and we found similar results. We can summarize our results by saying that, if one uses potentials that reproduce ground state properties and nucleon-nucleus elastic scattering data, the uncertainties related to the choice of single particle wave functions is about the 10%.

3.1. The Δ currents

The two-nucleon emission induced by two-body currents, for inclusive electron scattering processes, has been investigated in [9]. The results presented in that article indicate that the emission of two-like nucleons is a small contribution to the total, inclusive, cross section. In our case, however, it is important to know the relevance of the two-proton emission induced by Δ currents with respect to that induced by the SRC. There are two questions we would like to address in this part of the paper. The first one is about our capacity of describing the Δ currents, and the second one is about the possibility of finding particular kinematics able to minimize their effects.

In Fig. 4 we show the ^{16}O(γ,pp)^{14}C cross sections as a function of the θ_1 angle, for the final states indicated in Table 1. The cross sections have been calculated for ω=100 MeV, ϵ_2=40 MeV, and $\theta_2 = 0^o$. The calculations have been done considering only the Δ currents, i.e. there is not interference with the contribution of the SRC. The three curves of each panel have been obtained with different values of the $f_{\gamma N\Delta}$ and $f_{\pi N\Delta}$ coupling constants used in the evaluation of the diagrams of Fig. 2. A discussion of the validity of the various parameterizations is out of the scope of our work, we simply want to investigate the uncertainty produced on our results. The values we have used are taken from [9] (AMA), [27] (GIU), [28] (RYC), and they are given in Table 2. While the shapes of the angular distributions are not affected, the sizes of the cross sections are strongly modified by the various choices of the parameters.

The uncertainty on the global result depends from the interference between Δ currents

	AMA	GIU	RYC
$f_{\gamma N\Delta}$	0.299	0.373	0.120
$f_{\pi N\Delta}$	1.69	2.15	2.15

Table 2. Values of the parameters used in the evaluation of the Δ currents contribution. The AMA, GIU and RYC values are from Refs. [9], [27] and [28], respectively.

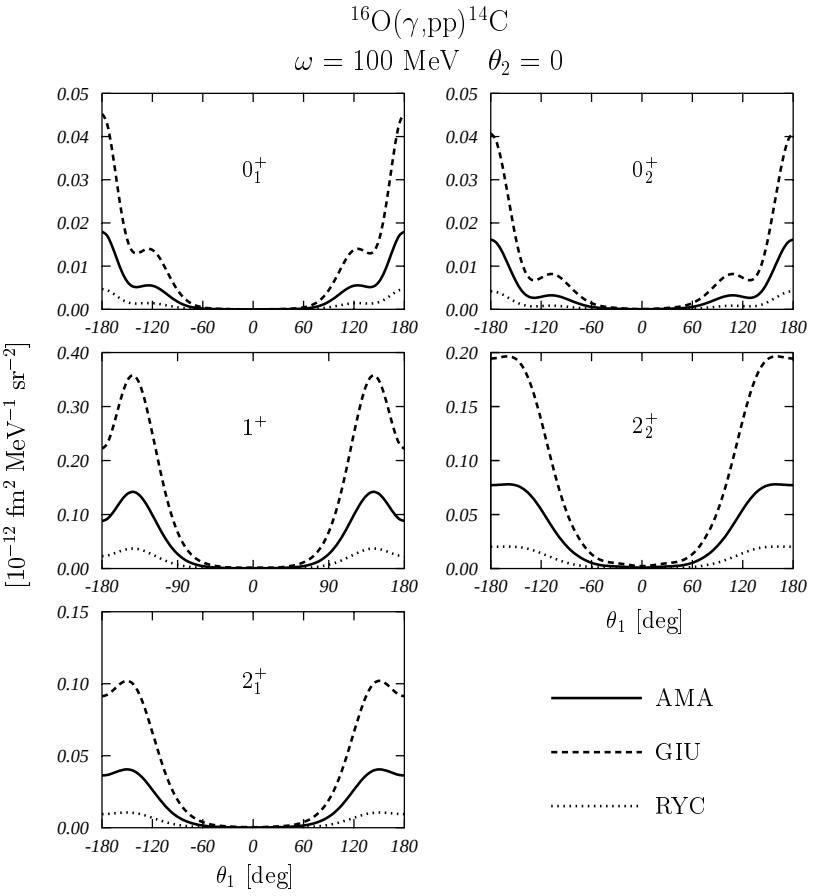

Figure 4. Cross sections angular distributions, as a function of θ_1, calculated with different parameterizations of the Δ coupling constants (see Table 2). The calculations have been done considering the Δ currents only and with ϵ_2=40 MeV. The labels of the various panels indicate the final states.

and SRC. In Fig. 5 we show the cross section angular distributions for the same kinematics of Fig. 4, and also for $\theta_2 = 60^o$, when the SRC are considered (the correlation function is the gaussian correlation we shall present in section 3.2). The results of Fig. 5 show that the differences between the various curves are rather small, apart from the case of 0_1^+ state at 60^o. By integrating in θ_1 the cross sections, as indicated in Eq. (12), we obtain a maximum difference of 10%, between the various calculations, with the exclusion of the case mentioned above where the differences can reach the 45%.

As indicated in [9] the effects of the Δ currents increase when the excitation energy becomes closer to the peak of the of the Δ resonance. This is evident from Fig. 6 where we show the ratios between the θ_1 integrated cross sections S defined in Eq. (12), calculated by using SRC only, $S(C)$, and by including also the Δ currents $S(C\Delta)$. The process investigated is ^{16}O(γ,pp)^{14}C, calculated for various values of θ_2 by using ϵ_2=40 MeV, for different final states of ^{14}C and for two different photon energies, 100 and 215 MeV. These two energy values have been chosen to be far from the giant resonance region, to minimize collective phenomena (see the discussion in [5]).

The smaller is the ratio the larger is the effect of the Δ currents. The general behaviour of the results shown in the figure confirms what was expected, i.e. the effects of the Δ

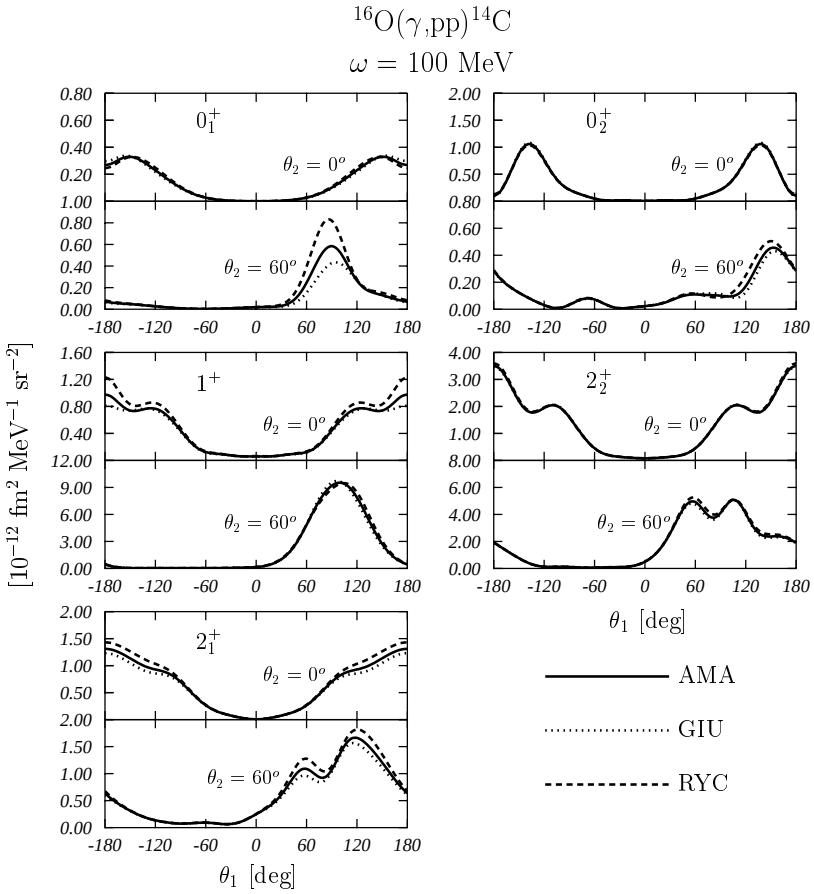

Figure 5. Cross sections angular distributions, as a function of θ_1, calculated with different parameterizations of the Δ coupling constants (see Table 2). All the calculations have been done with ϵ_2=40 MeV. The labels of the various panels indicate the final states and the values of θ_2.

currents are smaller at 100 MeV than at 215 MeV. More quantitative statements are difficult to make because of the strong dependence of the results from both the final state and θ_2. The behaviour of the 0_1^+ and 1^+ results at $\omega = 215$ MeV are quite anomalous with respect to those of the other results at the same energy. It is also worth to notice, in the case of ω=100 MeV, the peculiar results for the 0_1^+ final state at 60^o and 90^o.

Apart from the cases mentioned above, all the ratios calculated at $\omega = 100$ MeV are very close to the unity, showing a small effect of the Δ currents. The study of (e,e'pp) reactions done in [6] shows larger effects of the Δ currents, especially if one consider the case of the 1^+ state. A possible source of this difference can be related to the different values of the momentum transfer in photo and electron reactions. We have calculated the transverse response of Eq. (4) for various values of $|\mathbf{q}|$. In Fig. 7 we show the ratio

$$R = \frac{\int \mathrm{d}\theta_1 \sin\theta_1 w_t^C(|\mathbf{q}|)}{\int \mathrm{d}\theta_1 \sin\theta_1 w_t^{C\Delta}(|\mathbf{q}|)} \tag{13}$$

for the excitation energies and states considered before. The responses w_t^C have been calculated with SRC only, and $w_t^{C\Delta}$ by including also the Δ currents. The calculations

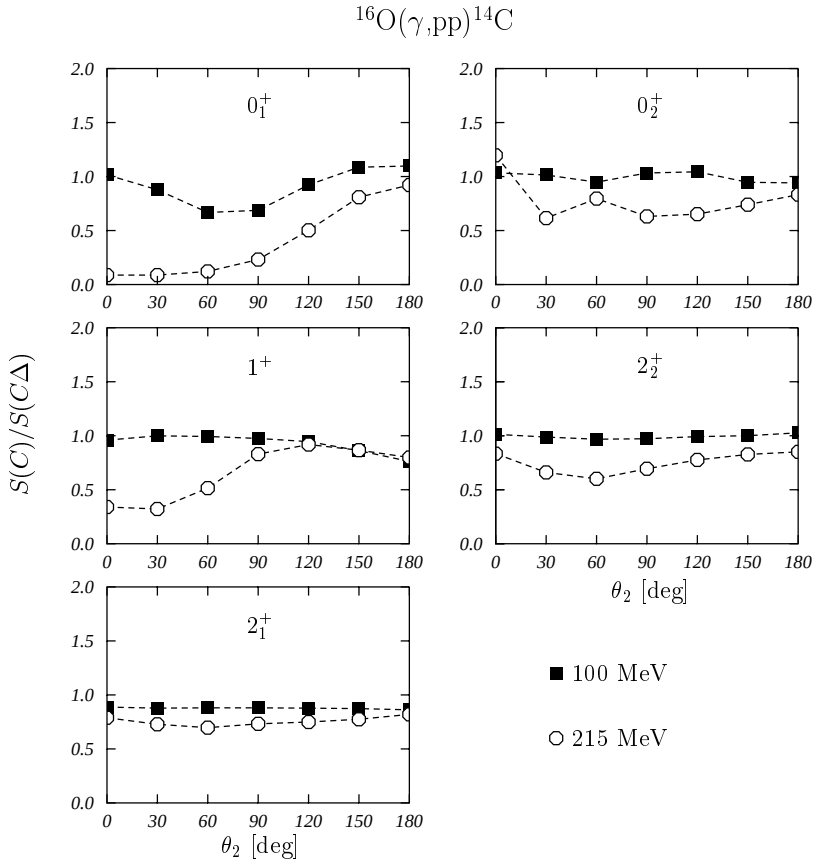

Figure 6. Ratio $S(C)/S(C\Delta)$, see Eq. (12), calculated for various values of θ_2 and for photon energies of 100 and 215 MeV. The calculations have been done with ϵ_2=40 MeV. The dashed lines have been drawn to guide the eyes.

have been done for $\theta_2 = 0^o$ and ϵ_2=40 MeV.

The figure shows that the contribution of the Δ currents increases with increasing value of $|\mathbf{q}|$. Also this general trend has an exception: the 0_2^+ at $\omega = 100$ MeV. It is however relevant the fact that, for all the considered cases, the value of the ratio at $\omega = 100$ MeV is very close to unity at the photon point. This indicates that the two-body Δ currents do not contribute significantly for photons.

In searching for kinematics set ups where the Δ currents contributions are rather small, we have investigated with some detail the case of the superparallel back-to-back case, which is one of the preferred situations from the experimental point of view. In Fig. 8 we show the cross sections for the ^{16}O(γ,pp)^{14}C reactions. The calculations have been done for $\omega = 100$ MeV, $\theta_2 = 180^o$ and $\theta_1 = 0^o$. The value of $|\mathbf{p}_r|$ has been defined as in Fig. 3, and it has been changed by modifying ϵ_2. The dashed lines have been obtained with SRC only, and the full lines contain also the Δ currents. The results of the two calculations are rather similar, showing again the scarce relevance of the Δ currents at ω=100 MeV. The only remarkable difference between calculations with and without Δ currents appears for the 0_1^+ final state in the region of the high positive values of $|\mathbf{p}_r|$.

These conclusions are not a special feature related to the chosen kinematics but they represent a general trend. In Fig. 9 the squares show the ratios between the S factors (Eq. 12)

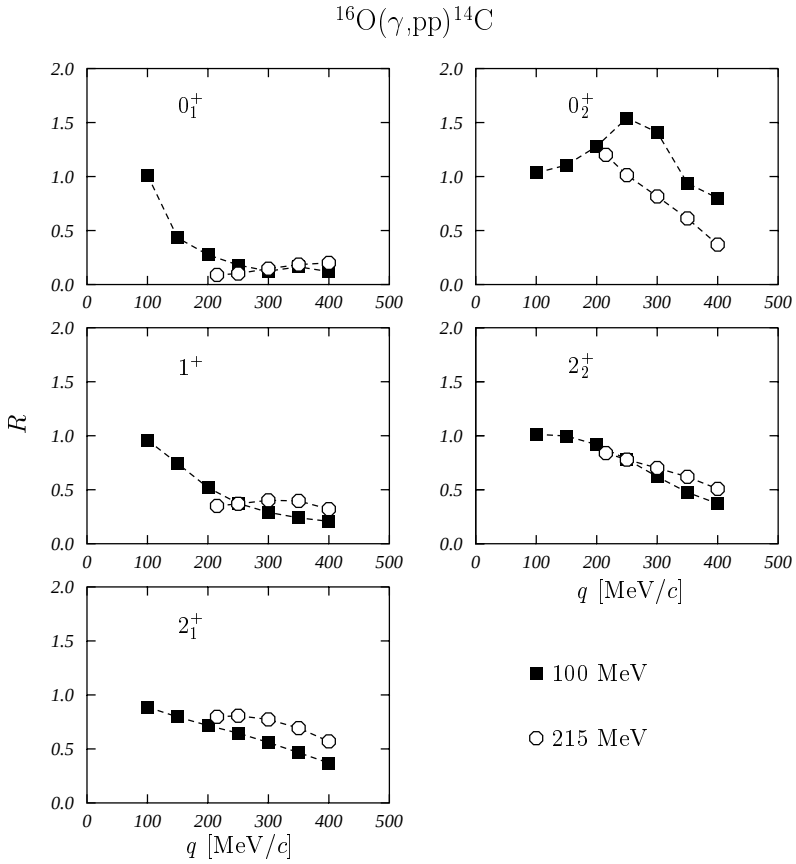

Figure 7. Ratio between the integrated $w_t(|\mathbf{q}|)$ responses calculated without and with Δ currents, see Eq. (13). The ratios have been calculated for $\theta_2 = 0^o$.

calculated without and with Δ currents as a function of ϵ_2 (black squares). In the same figure, the ratios between the superparallel cross sections of Fig. 8, calculated without and with Δ currents are shown by the open circles. In general the two ratios are very similar, and this indicates that the Δ currents are not suppressed in superparallel kinematics. Remarkable the behaviour of the 0_2^+ for large ϵ_2 values. This is related to some peculiarity of the superparallel kinematics as we shall discuss in the next section.

The results we have just discussed do not imply that the Δ currents are always negligible. It possible to find specific kinematics where they become more important than the SRC. As example, we show in Fig. 10 the results obtained for the 0_1^+ state for the ^{16}O(γ,pp)^{14}C reaction in symmetric kinematics. This kinematics consists in setting $\theta_1 = \theta_2$, and $\epsilon_1 = \epsilon_2 = 0.5(\omega - \epsilon_{h_1} - \epsilon_{h_2})$. The figure shows that, in this case, the Δ currents play an important role at both photon energies considered.

3.2. The correlations

The main goal in the study of the two nucleon emission processes regards the possibility of obtaining information about SRC. We conducted this investigation by comparing the results obtained with different SRC.

All the results presented up to now have been obtained by using a gaussian correlation

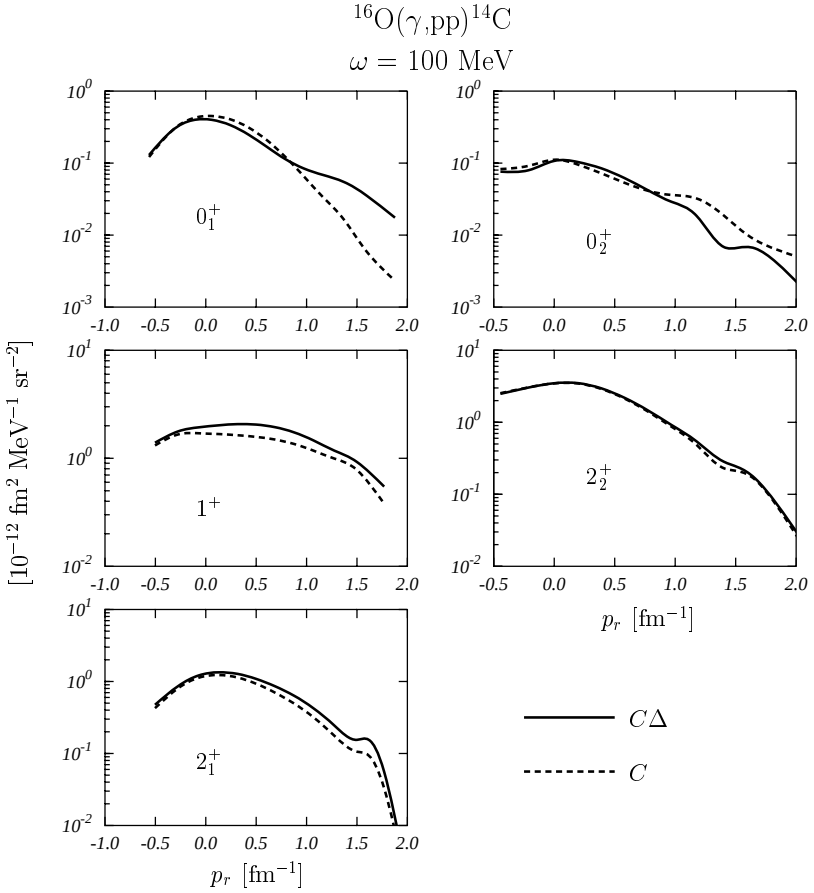

Figure 8. Cross sections in superparallel back to back kinematics with $\theta_2 = 180^o$. The variable $|\mathbf{p}_r|$ has been defined, and changed, as in the panel (c) of Fig. 3. The full lines have been obtained by considering both SRC and Δ terms, while the dashed lines show the results obtained without the Δ terms.

of the type

$$f(r) \, = \, 1 \, - \, a \, \exp\left(-br^2\right) \, , \tag{14}$$

with $a = 0.7$ and $b = 2.2$ fm^{-2}. These values have been fixed in [25] by minimizing the energy functional for nuclear hamiltonian containing the Afnan and Tang nucleon-nucleon interaction [29]. This calculation has been done in the framework of the Correlated Basis Function theory by using Fermi Hypernetted Chain resummation techniques.

Within the same theoretical approach, the other two correlations have been fixed by using a method called Euler procedure [30]. With this procedure the SRC depend only from a single parameter, the healing distance, whose value is also fixed by a minimization the energy functional. The correlation function labeled $S3$ in the figure is obtained in this way [25] when the Afnan and Tang nucleon-nucleon interaction is used in Fermi Hypernetted Chain calculations of the doubly magic nuclei ^{12}C, ^{16}O, ^{40}Ca, ^{48}Ca and ^{208}Pb. The other correlation function we have adopted in our calculation, labeled $V8$ in the figure, is the scalar term of the state dependent correlation used in [31] for the Fermi Hypernetted Chain calculations of the ^{16}O and ^{40}Ca nuclei done with the V8' parameterization of the realistic

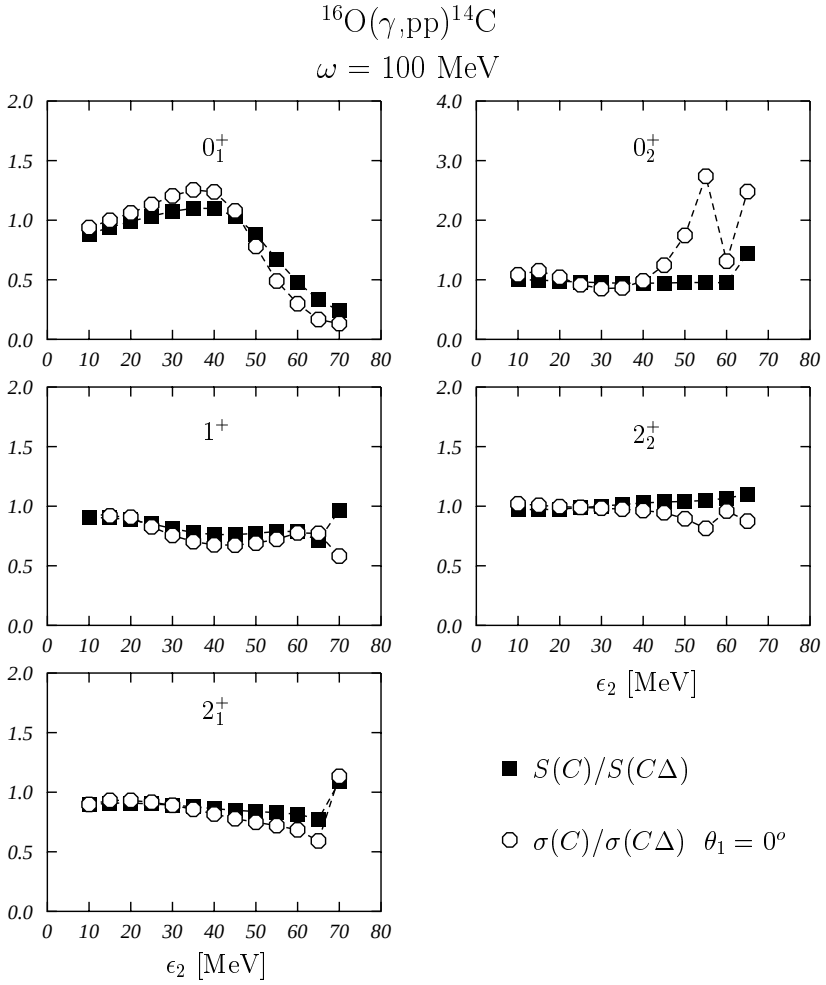

Figure 9. The squares show the ratios between the S factors of Eq. (12) calculated without and with Δ currents respectively. The circles show the ratios of the cross sections of superparallel kinematics shown in Fig. 8 calculated with and without delta. The ratios are shown as a function of the energy ϵ_2, and they have been calculated with $\theta_2 = 180^o$.

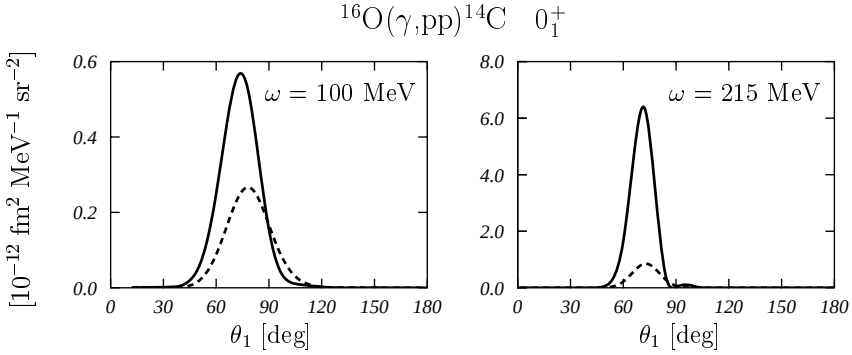

Figure 10. Cross section angular distributions for the 0_1^+ final state in ^{14}C in symmetric kinematics (see sect. 3.2). The full lines show the results obtained by considering both SRC and Δ-currents. The results shown by the dashed lines have been obtained with SRC only.

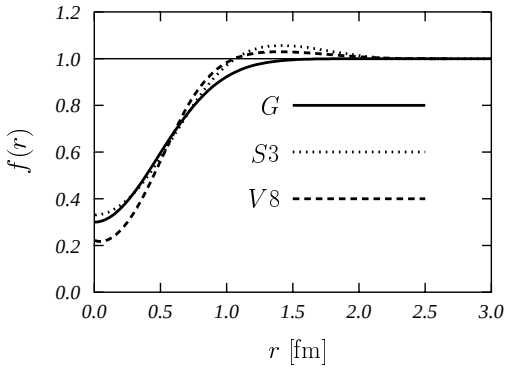

Figure 11. Correlation functions used in our calculations as a function the relative distance between the nucleons. The line labeled G and $S3$ indicate the gaussian and Euler correlations of [25]. With $V8$ we show the scalar term of the state-dependent correlation of [31].

Argonne V18 nucleon-nucleon potential [32] plus the Urbana IX three-body interaction [33]. As it is shown in Fig. 11 the three SRC differ for few details. The $V8$ and $S3$ correlations become larger than the asymptotic value of 1 in the region between 1 and 2 fm. The $V8$ correlation has a lower minimum than the other two.

We have studied the (γ,pp) reaction for ^{12}C, ^{16}O and ^{40}Ca target nuclei. As example of the obtained results, we show in Fig. 12 some cross section angular distributions. The results of the figure have been obtained for final states leading to the ground state of the A-2 nuclei, with θ_2=90^o and ϵ_2=40 MeV. The shapes of the angular distributions are not strongly modified by the various correlations. The main difference between the various results is in the size of the cross section.

To have concise information from our calculations we have evaluated the S factors of Eq. (12), for all the states of Table 1, for ϵ_2=40 MeV and for θ_2 = 0^o, 30^o, 60^o, 90^o, 120^o, 150^o and 180^o. We show in Table 3 the ratios between the S factors calculated with $S3$ and $V8$ and those calculated with the gaussian correlation averaged on the θ_2 variable. In the table the uncertainty on the average is calculated as a standard deviation.

All the values given in the table are smaller than one, and this indicates that the gaussian correlation produces the largest cross sections. In general, the $V8$ cross sections are larger

	^{12}C		^{16}O		^{40}Ca	
	$S3$	$V8$	$S3$	$V8$	$S3$	$V8$
0^+_1	0.73 ± 0.11	0.52 ± 0.05	0.10 ± 0.11	0.20 ± 0.05	0.15 ± 0.03	0.22 ± 0.04
0^+_2			0.83 ± 0.16	0.60 ± 0.08	0.37 ± 0.07	0.44 ± 0.07
1^+			0.97 ± 0.08	0.76 ± 0.07	0.37 ± 0.04	0.36 ± 0.06
2^+_1	0.56 ± 0.13	0.52 ± 0.08	0.25 ± 0.05	0.30 ± 0.04	0.22 ± 0.05	0.24 ± 0.03
2^+_2			0.54 ± 0.13	0.52 ± 0.08	0.54 ± 0.07	0.48 ± 0.05

Table 3. Ratios between the S factors calculated with the $S3$ and $V8$ correlations and those calculated with the Gaussian correlation, averaged on the θ_2 variable (see sect. 3.2).

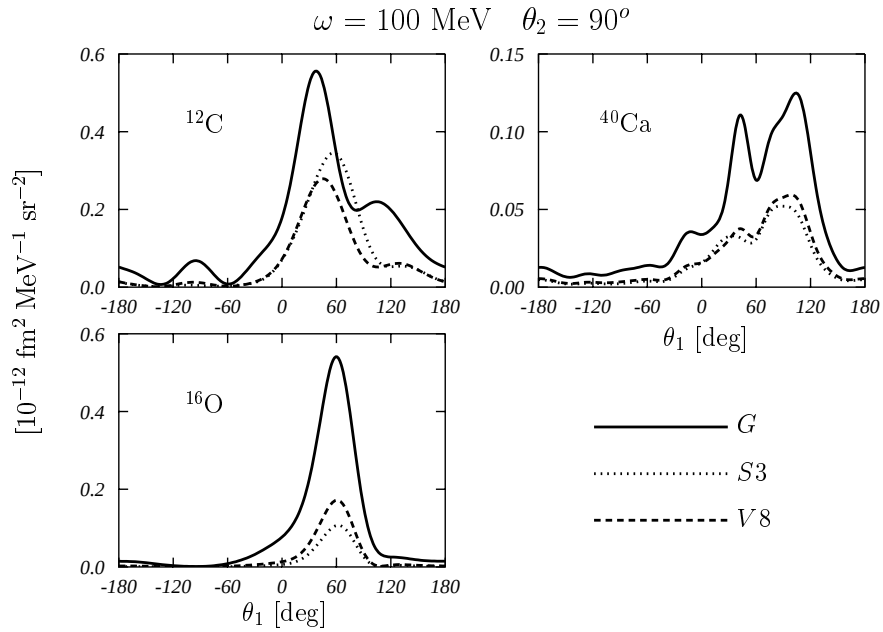

Figure 12. Angular distributions of the (γ,pp) cross sections for the three different nuclei considered. The kinematics variables have been fixed as ω = 100 MeV, $\theta_2 = 90^o$ and ϵ_2=40 MeV. The final states are the ground states of the A-2 nuclei, which correspond to the 0^+_1 states of Table 1. The full lines have been obtained with the gaussian correlation, the dotted ones with the $S3$ correlation and the dashed lines with the $V8$ correlation.

than those obtained with the $S3$ correlation. Analogous results have been obtained in [6]. In that reference, it has been shown that the behaviour of the $S3$ and $V8$ correlation functions in the region of 1-2 fm where they assume values larger than one, has opposite effect with respect to that of the region at smaller r values. Gaussian and $S3$ correlation functions have the same minimum, but the gaussian correlation does not have the overshooting of the asymptotic values. For this reason the cross sections obtained with the gaussian correlation are larger than the other ones. The $V8$ correlation function has a smaller minimum, and also its overshooting values in the 1-2 fm region are smaller than those of the $S3$ correlation function.

These general features of our results, obtained by making angular integrations and averages, are not respected in every kinematic situation. The cross sections strongly depend upon all the kinematic variables, from the nuclear final states up to the angles and the energies of the two emitted protons. As an example of this sensitivity we show in Fig. 13 the ^{16}O(γ,pp)^{14}C cross sections calculated for various final states in superparallel back-to-back kinematics. As before, the variable $\mathbf{p}_r$ has been changed by changing the energy ϵ_2, and consequently ϵ_1.

Also in this case we observe that the general behaviour emerging from the study of Table 3 is respected. The cross sections calculated with the gaussian correlation are the largest ones. The 0^+_2 results show an opposite behaviour. The largest cross sections are those produced by the $S3$ correlation, and the smallest ones by the gaussian correlation. To understand better the source of the of this difference we show in Fig. 14 the angular distributions of the ^{16}O(γ,pp)^{14}C cross sections for the 0^+_2 final state. The cross section values used for the

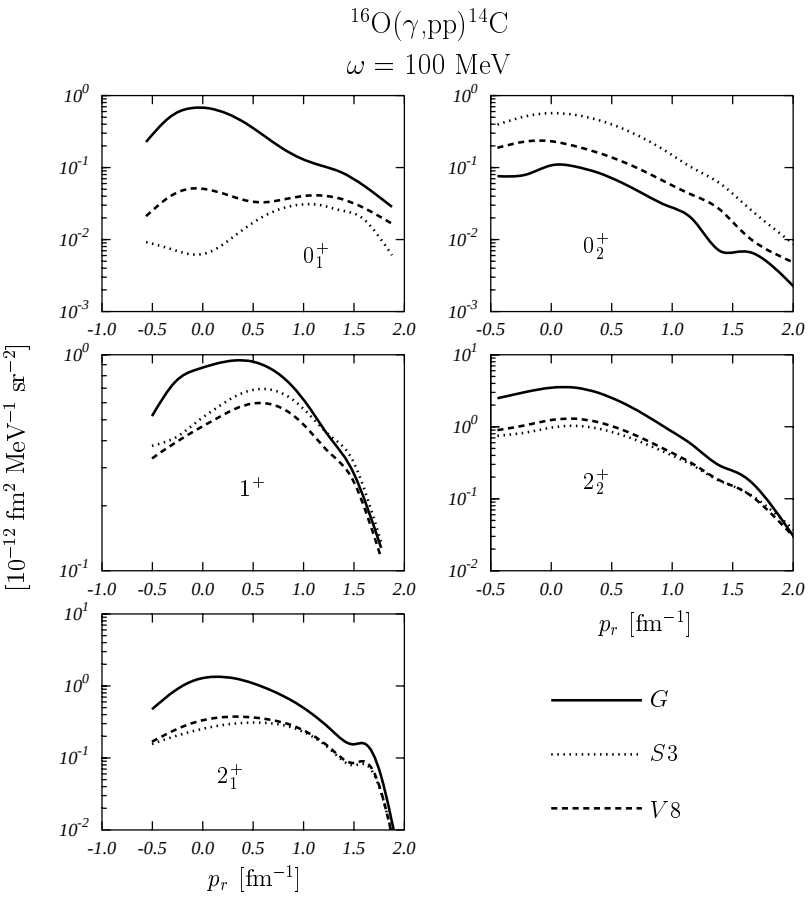

Figure 13. ^{16}O(γ,pp)^{14}C cross sections calculated for various final states in superparallel back to back kinematics ($\theta_1 = 0^o$,$\theta_2 = 180^o$). The variable $|\mathbf{p}_r|$ has been defined, and changed, as in Fig. 3.

superparallel back-to-back results are those at θ_1=0^o where the $S3$ cross sections are larger than the other ones. On the other hand the figure clearly shows that the largest values of the angular integrated cross sections are those obtained with the gaussian correlation.

The shapes of the angular distributions shown in Fig. 14 resemble those of the (e,e'p) experiments when the emitted particle is coming from a bound p wave, with the typical minimum at the origin [16]. The (γ,pp) cross section is related to the wave function describing the motion of the correlated pair in target nucleus ground state [7]. This is the combined wave function of the two-particles with respect to the nuclear center. Clearly the result depends also from the correlation used, as the different lines of Fig. 14 show. In any case the typical p wave behaviour is present in all the cases. Also the $S3$ results start to show the characteristic minimum at the origin when the kinematics allows to probe small values of the relative momentum of the correlated hole pair. This behavior of the $S3$ response function is also shown in Fig. 15 where the angular distributions of the $w_t(|\mathbf{q}|)$ responses are shown as a function of θ_1 for different values of $|\mathbf{q}|$. This manner of changing the kinematics cannot be achieved in photo emission, but in electron scattering. The figure shows that for certain values of $|\mathbf{q}|$ the angular distributions have a minimum at the origin.

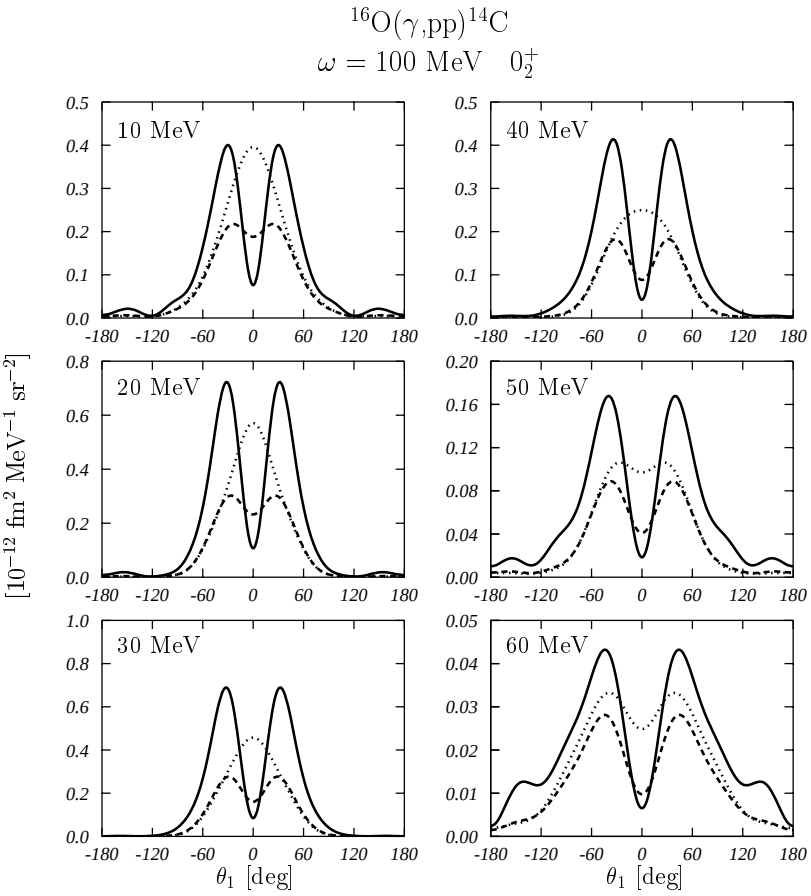

Figure 14. Angular distributions of the ^{16}O(γ,pp)^{14}C cross sections for the 0_2^+ final state. The energy values in the various panels correspond to ϵ_2. The meaning of the lines is analogous to that of Fig. 13: full, dotted and dashed lines correspond to the G, $S3$ and $V8$ correlations, respectively.

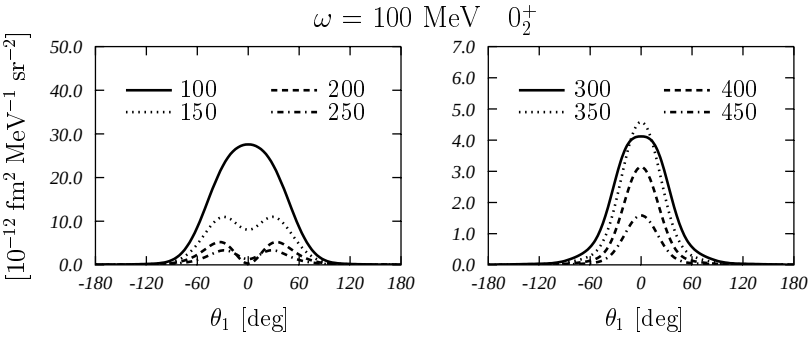

Figure 15. Response functions $w_t(\mathbf{q})/|\mathbf{p}_1|^2|\mathbf{p}_2|^2$ for the emission of two protons from ^{16}O calculated with the $S3$ correlation function for $\theta_2 = 180^o$ and $\epsilon_2 =$ 40 MeV. The labels explaining the meaning of the lines indicate the values of $|\mathbf{q}|$ in MeV/c.

4. Summary and conclusions

In this paper we have applied to the (γ,pp) reaction the model developed in [1, 2, 3, 4, 5]. We first analyzed the sensitivity of our results to the uncertainties related to the choices of the mean field potentials describing the single particle wave functions. Hole and particle wave functions are generated by two different potentials whose parameters are fixed by using different criteria. The hole wave functions should describe some property of the target nucleus ground state, for example charge distributions and single particle energies. The particle wave functions are generated by optical potentials that reproduce the elastic nucleon-nucleus cross sections. The use of various potentials, all of them satisfying these criteria, produces variations of few percent on the cross section.

We have conducted a study on the relevance of the Δ currents on the cross section, since they are the only mechanism, competing with SRC, able to emit two protons. The uncertainty on the values of the coupling constants produces large effects on the Δ currents (see Fig. 4). Fortunately the contribution to the cross section of the Δ currents is, in general, smaller than that of the SRC. Therefore this uncertainty affects the cross section values at the 10% level. Because of the large number of kinematic variables into play this result should be more carefully stated. As expected, the Δ currents are small in the region far from the peak of the Δ resonance, and become relatively larger while approaching it (see Fig. 6). On the other hand, we have shown in Fig. 7, that at fixed nuclear excitation energy, the relative effect of the Δ currents increases with increasing momentum transfer. For this reason the Δ currents affect more the (e,e'pp) processes than the (γ,pp) reactions.

The choice of the kinematics could modify these results. We analyzed superparallel back-to-back kinematics and found that they reproduce the general trend obtained by integrating on the angular distribution of one of the emitted protons (see Figs. 8 and 9). On the other hand, in a different kinematics, the symmetric one, the Δ currents become more important than the SRC (see Fig. 10).

The sensitivity of the cross section to the details of the correlation has been studied by using three different correlation functions, shown in Fig. 11. The calculations have been done for the ^{12}C, ^{16}O and ^{40}Ca nuclei. The various correlations do not sensitively modify the shapes of the angular distributions, but they modify the the size of the cross section. We observe that the overshooting of the asymptotic value of the correlation function produces a lowering of the cross section. In general the results obtained with the gaussian correlation, which does not have that overshooting, are larger than those obtained with the other correlations.

Also in this case this general behaviour strongly depends on the kinematics. We have shown in Fig. 13, that for a specific case in superparallel back-to-back kinematics, the gaussian results are the smaller ones. The study of this special case has shown that the shapes of the angular distributions are strongly related to the wave function of the correlated proton pair before being emitted. Choosing special points of this angular distributions could be misleading on the general behaviour of the cross sections.

Our study shows that the behaviour of the (γ,pp) cross sections analyzed in terms of angular distribution of one of the emitted protons, can be rather well interpreted in terms of SRC. We have shown that the cross sections follows a well controlled behaviour if, after fixing the angle of one of the emitted protons, one analyzes the complete angular distribution of the other proton. A selection of specific kinematics, such as the symmetric or superparallel ones, could provide results out of the systematics. The evident experimental limitations with respect to a full 4 π coverage of the angular distribution, implies some specific kinematics to be selected. It is therefore necessary a joint work between experimentalists and theoreticians

to analyze the peculiarities of the chosen kinematics.

The above considerations can be applied also to the (e,e'pp) reactions. There are, however, two features making the emission of two protons induced by real photon a better tool for the study of the SRC. First, in the photon case the longitudinal response is not present, therefore the analysis of the angular distributions is simplified. Second, the $\mathbf{q}$ dependence of the Δ currents is such that their minimum contribution is at the photon point.

Acknowledgments

We thank Carlotta Giusti for her interest in our work and the numerous discussions. This work has been partially supported by the agreement INFN-CICYT, by the DGI-FEDER (BFM2002-03218), by the Junta de Andalucia (FQM 220) and by the MIUR through the PRIN *Fisica del nucleo atomico e dei sistemi a molticorpi*.

References

[1] G. Co', A.M. Lallena, Phys. Rev. C 57 (1998) 145
[2] S.R. Mokhtar, G. Co', A.M. Lallena, Phys. Rev. C 62 (2000) 067304
[3] G. Co', A.M. Lallena, Ann. Phys. (N.Y.) 287 (2001) 101
[4] S.R. Mokhtar, M. Anguiano, G. Co', A.M. Lallena, Ann. Phys. (N.Y.) 292 (2001), 67
[5] M. Anguiano, G. Co', A.M. Lallena, S.R. Mokhtar, Ann. Phys. (N.Y.) 296 (2002), 235
[6] M. Anguiano, G. Co', A.M. Lallena, J. Phys. G 27 (2003) 2109
[7] C. Giusti, F.D. Pacati, K. Allaart, W.J.W. Geurts, W.H. Dickhoff, H. Müther Phys. Rev. C 57 (1998) 1691
C. Giusti, F.D. Pacati, Nucl. Phys. A 641 (1998) 297
[8] J. Ryckebusch, D. Debruyne, W. Van Nespen, Phys. Rev C 57 (1998) 1319
[9] J.E. Amaro, G. Co', A.M. Lallena, Nucl. Phys. A 578 (1994) 365
[10] A.M. Lallena, Nucl. Phys. A 615 (1997) 325
[11] R.C. Carrasco, E. Oset, Nucl. Phys. A 536 (1992) 445;
R.C. Carrasco, M.J. Vicente-Vacas, E. Oset, Nucl. Phys. A 570 (1994) 701
[12] C. Giusti, F.D. Pacati, M. Radici, Nucl. Phys. A 546 (1992) 607;
S. Boffi, C. Giusti, F.D. Pacati, M. Radici, Nucl. Phys. A 564 (1993) 473;
P. Wilhelm, H. Arenhövel, C. Giusti, F.D. Pacati, Zeit. Phys. A 359 (1997) 467;
C. Giusti, F.D. Pacati, Nucl. Phys. A 641 (1998) 297
[13] M. Schwamb, S. Boffi, C. Giusti, F.D. Pacati, Eur. Phys. J. A20 (2004) 233.
[14] M. Vanderhaeghen, L. Machenil, J. Ryckebusch, M. Waroquier, Nucl. Phys. A 580 (1994) 551;
J. Ryckebusch, L. Machenil, M. Vanderhaeghen, V. Van der Sluys, M. Waroquier, Phys Rev. C 49 (1994) 2704
[15] M. Kanazawa et al., Phys. Rev. C 35 (1987) 1828;
G.E. Cross et al., Nucl. Phys. A 593 (1995) 463;
E.D. Hackett et al., Phys. Rev. C 53 (1996) R1047;
P.D. Harty et al., Phys. Lett. B 380 (1996) 247;
I.J.D. MacGregor et al., Phys. Rev. Lett. 80 (1998) 3146;
T.T.-H. Yau et al., Eur. Phys. J. A 1 (1998) 241;
S.J.D. McAllister et al., Phys. Rev. C 60 (1999) 044610;
L. Isaksson et al., Phys. Rev. Lett. 83 (1999) 3146;
S. Franczuk et al., Phys. Lett. B 450 (1999) 332;
D.P. Watts et al., Phys. Rev. C 62 (2000) 014616.
[16] S. Boffi, C. Giusti, F.D. Pacati, M. Radici, *Electromagnetic Response of Atomic Nuclei* (Clarendon Press, Oxford, 1996).

[17] G. Hoehler et al. Nucl. Phys. B 114 (1976) 505
[18] Th. Wilbois, P. Wilhelm, H. Arenhövel, Phys. Rev. C 54 (1996) 3311
[19] S. Fantoni, V.R. Pandharipande, Nucl. Phys. A 473 (1987) 234
[20] G. Co', Nuov. Cim. A 108 (1995) 623
[21] F. Arias de Saavedra, G. Co', M.M. Renis, Phys. Rev. C 55 (1997) 673
[22] J.E. Amaro, A.M. Lallena, G. Co', A. Fabrocini, Phys. Rev. C 57 (1998) 3473
[23] P. Schwandt et al., Phys. Rev. C 26 (1982) 55
[24] A. Nadasen et al., Phys. Rev. C 23 (1981) 1023
[25] F. Arias de Saavedra, G. Co', A. Fabrocini, S. Fantoni, Nucl. Phys. A 605 (1996) 359
[26] S. Boffi, F. Cannata, F. Capuzzi, C. Giusti, F.D. Pacati, Nucl. Phys. A 379 (1982) 509
[27] C. Giusti, F.D. Pacati, Nucl. Phys. A 615 (1997) 373
[28] J. Ryckebusch, V. Van der Sluys, K. Heyde, H. Holvoet, W. Van Nespen, M. Waroquier, M. Vanderhaeghen, Nucl. Phys. A 624 (1997) 581
[29] I.R. Afnan, Y.C. Tang, Phys. Rev. 175 (1968) 1337.
[30] G. Co', A. Fabrocini, S. Fantoni, I. Lagaris, Nucl. Phys. A 549 (1992) 439
[31] A. Fabrocini, F. Arias de Saavedra, G. Co' Phys. Rev. C 61 (2000) 044302
[32] R.B. Wiringa, V.G.J. Stoks, R. Schiavilla, Phys. Rev. C 51 (1995) 38
[33] B.S. Pudliner, V.R. Pandharipande, J. Carlson, S.C. Pieper, R.B. Wiringa, Phys. Rev. C 56 (1997) 1720